

Validation of an approach to analyse and understand ship wave making

Hoyte C. Raven

Received: 2 January 2010 / Accepted: 16 June 2010 / Published online: 7 August 2010
© JASNAOE 2010

Abstract This paper discusses a rational and systematic procedure for understanding and analysing steady ship wave patterns and their dependence on hull form. A step-wise procedure is proposed in which the pressure distribution around the hull is invoked to provide a qualitative understanding of the connection between hull form and wave making. In a recent publication it was shown how this understanding explains various known trends and, in combination with wave pattern computations by free-surface potential flow or Reynolds-averaged Navier–Stokes (RANS) methods, can often be exploited to reduce wave making by modifying the hull form. The present paper provides support for the guidelines given, validates the decomposition into different steps and indicates the connection with previous theoretical approaches.

Keywords Ship waves · Slow-ship linearisation · Hull form design

1 Introduction

This is perhaps a somewhat unusual paper. We address one of the fundamental issues in ship hydrodynamics: the relation between ship hull form and the wave pattern it generates. However, rather than proposing a new prediction method or a specific application, we offer an approach that helps to understand this relation, which is essential to design a ship hull form such that it has low wave

resistance. The paper discusses and validates a way of working and general insights. We go back to simple linear potential theory for steady ship waves, and base ourselves on well-known textbook material. However, to the best of the author's knowledge, that material has rarely, if ever, been presented in this context, and the proposed procedure based on it does not seem to be widely known. Therefore, we hope that the present paper may be of practical use for many.

Obviously, for ship performance, wave making is just one of the aspects; viscous resistance, wake field and propulsion efficiency also play important roles. However, separate consideration of wave making is still quite relevant, as reduction of wave resistance can often be achieved without unduly affecting the viscous resistance or wake field. Moreover, while wave resistance is usually not the largest resistance component for a merchant ship, in many cases it is the component that is most easily reduced by proper modifications to the hull form. This is an opportunity and a challenge at the same time. How should these modifications be determined?

In the past, resistance reductions were targetted in a model testing program. A model of an initial hull form was towed, its resistance measured, and the wave pattern was observed by an experienced naval architect. Hull form modifications were then proposed based on experience, on intuition and to some extent on 'trial and error'. Several models were often built for a single project, making the procedure rather time-consuming and costly.

Extensive research in the last century has led to several theoretical wave resistance prediction methods intended for use in ship design. A variety of linearised methods have been proposed, in which originally also the hull boundary conditions were linearised (thin-ship, flat-ship, slender-body methods), but later only the free-surface boundary

H. C. Raven (✉)
Maritime Research Institute Netherlands (MARIN),
P.O. Box 28, 6700 AA Wageningen, The Netherlands
e-mail: h.c.raven@marin.nl

conditions (Neumann–Kelvin, slow-ship). A strong impetus was provided by the introduction of various slow-ship theories, which appeared to provide better resistance predictions than earlier methods. One practical and widespread method of this class was that proposed by Dawson in 1977 [1], which has been used in ship design for some time.

Around 1990 a major step was made in the theoretical development, with the introduction of complete nonlinear free-surface potential flow codes [2–5]. These methods produce much more accurate predictions, and their use in design is widespread now. One of these codes will be used in this paper for studying trends and validating guidelines.

Nevertheless, these codes do not design a ship, but rather enable evaluation of a given design. It is the designer who decides on the required hull form modifications, and the problem is still how to derive proper design adjustments that lead to a reduction of wave resistance.

If one has a tool that predicts the wave resistance of a ship hull form exactly, the best approach to design for minimum wave resistance could be a formal optimisation technique. This requires that a wave resistance prediction tool be linked to an optimiser and a parametric hull form variation tool. Several examples of such procedures have been published, e.g. [6–8]. However, in this context a very similar issue arises: how to choose parametric hull form variations offering the best prospect for wave resistance reduction. Without an answer to this, a vast number of hull form parameters need to be addressed, making the optimisation time-consuming and unclear.

To improve ship hull forms from a wave-making point of view, and to assess the quality of predictions and optimisations correctly, it is desired to understand how wave making is connected with features of the hull shape. This is a difficult question to answer in general. There are several simple guidelines on the best hull form for given speed ranges, rules of thumb for bulbous bow dimensions or transom height, indications on frame shapes etc. However, without further insight it is hard to understand these guidelines, to know when they apply or to move beyond what has been tried before.

Recently, an alternative approach has been described in the new issue of the ‘Ship Resistance and Flow’ volume of the *Principles of Naval Architecture* series [9]. This is a formalisation of a working procedure we have developed at MARIN in the course of many projects for shipyards over the years. It has been used in essence since 1988, initially using predictions from the DAWSON code [10] and later predictions from RAPID [5]. We assume that a computed wave pattern and flow field are available, and we analyse these to deduce what design changes are desired to reduce certain wave components. The analysis is based on decomposing the relation between hull form and wave making into simpler steps, and trying to understand those

separate steps. This understanding is loosely based on linear theory, is not always quantitatively precise, but if combined with computational predictions can lead to a successful and sound hull form improvement process.

The present paper briefly summarises the essence of this approach, but mainly it focusses on a discussion and validation of the trends and guidelines described, and on an inspection of the validity of the approach overall. Thus, it provides support for the simplified analysis, and in addition casts an interesting light on the validity of certain older slow-ship wave-making theories.

The paper is organised as follows. First we give a brief outline of the wave resistance prediction code that has been used to generate the examples provided, and we briefly recall a relevant part of basic ship wave theory. In Sect. 4 we outline the separate steps made and the guidelines for each. Section 5 then provides a discussion of each step, and gives illustrations of the guidelines. Section 6 discusses the relation of the present stepwise procedure with earlier ship wave theories, then some examples are given of the validity of the procedure in practice. Finally, we discuss some examples of the application of the approach to aspects of hull form design, and draw conclusions.

2 Wave pattern computations

For the methodology discussed below the particular flow code used is rather immaterial, but for completeness we briefly indicate the method we have used to generate the wave patterns and flow fields shown. This is the free-surface potential flow code RAPID [5, 11], which solves the problem of the steady free-surface flow around a ship at constant forward speed in still water. It imposes exact inviscid, fully nonlinear free-surface boundary conditions, and takes into account the dynamic trim and sinkage of the vessel. The solution is obtained in an iterative procedure in which the wave elevation, flow field, trim and sinkage are repeatedly updated until a converged solution of the nonlinear problem has been found. In each iteration a linear problem is solved using a panel method. Source panel distributions are used on the hull surface and on a plane at a small distance above the wave surface. Both panellings are repeatedly updated during the iterative process. Typically we use 2000–3500 panels on one half of the hull surface and 4000–20000 on one half of the wave surface. For a complete calculation the computation time usually varies from a few minutes to half an hour on a standard single-processor personal computer. RAPID has been used in hull form design on a daily basis at MARIN since 1994, and in addition is used by several licencees worldwide (shipyards, navies and universities).

3 Ship waves

In our process to assess and minimise wave resistance, we will focus on the wave pattern generated by the ship in the first place, as it is far more informative than just a predicted wave resistance value. While the basic properties of ship wave patterns are described at length elsewhere, e.g. [9, 12], for reference we briefly recall some of the essential relations here.

We consider a ship in steady forward motion in still water. We use a frame of reference moving with the ship, with x pointing aft and z upward. In this system the wave pattern and the flow around the hull are steady. We make the usual assumption that wave making is dominated by inviscid-flow properties. Evidently, the generation of stern waves is affected by viscosity, but their propagation less so, and the general approach sketched below remains relevant. A potential-flow assumption can then be made, at least for the wave properties away from the hull surface. The velocity field is the gradient field of a scalar potential ϕ , which for incompressible flows satisfies the Laplace equation $\nabla^2\phi = 0$. The pressure is found from Bernoulli’s equation and consists of a hydrostatic pressure and a hydrodynamic contribution p_{hd} . The latter is the meaningful quantity in our case. It is nondimensionalised using the fluid density ρ and the ship speed V as:

$$c_p \equiv \frac{p_{hd}}{\frac{1}{2}\rho V^2} = 1 - \frac{\nabla\phi \cdot \nabla\phi}{V^2}. \tag{1}$$

Steady free-surface potential flow must satisfy free-surface boundary conditions, demanding that the pressure at the water surface is atmospheric, and that the wave surface is a streamsurface. These two boundary conditions are nonlinear. In the development of prediction methods for ship wave patterns, linearisations for small wave steepness have long been used, and while the resulting methods were usually not quite accurate, linear theory is most appropriate for providing an understanding of ship waves. Linearisation relative to the undisturbed uniform flow leads to the so-called Kelvin boundary condition:

$$Fn^2 \frac{\partial^2\phi}{\partial x^2} + \frac{\partial\phi}{\partial z} = 0, \tag{2}$$

in which $Fn = V/\sqrt{gL}$. This boundary condition is linear and homogeneous, and therefore admits superposition of solutions, just like the Laplace equation.

Specifically, a ship wave pattern, at least in the far field, can be approximated as a superposition of sinusoidal waves propagating over an undisturbed flow, so-called free waves. Properties of sinusoidal waves are easily derived from the Laplace equation and Kelvin condition. We readily find that the wave propagation speed c and the wave length λ are related by the well-known dispersion relation:

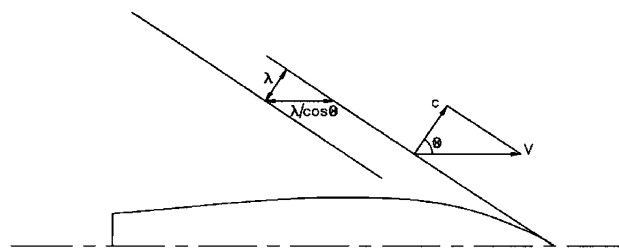


Fig. 1 Direction, phase speed and length of wave components in three-dimensional cases

$$\lambda = \frac{2\pi c^2}{g}. \tag{3}$$

For a two-dimensional steady case, e.g. a submerged cylinder at right angles to the flow moving with constant speed V through still water, the phase velocity of the steady two-dimensional (2D) waves must be equal to V , and from Eq. 3 we find $\lambda = 2\pi V^2/g = 2\pi Fn^2L$. So, far enough aft of the body, there is just a single wave component present.

In three-dimensional cases such as ships, there is an additional degree of freedom, which is the wave propagation direction, indicated as θ in Fig. 1. A local disturbance, such as the bow of a ship, can generate an infinite set of wave components propagating in various directions $-\pi/2 < \theta < +\pi/2$. In actual ship wave patterns, components with angles up to $\theta = 60^\circ\text{--}70^\circ$ can often be observed.

In order for waves to be steady in the coordinate system moving with the ship, the phase velocity must be $c = V \cos \theta$, and according to the dispersion relation

$$\lambda(\theta) = 2\pi c^2/g = 2\pi Fn^2L \cos^2 \theta. \tag{4}$$

The longest waves in the pattern are therefore the transverse waves, which have length $\lambda_0 = 2\pi Fn^2L$, the fundamental wave length. All other steady waves are shorter by a factor $\cos^2 \theta$. The distinction between transverse and diverging waves is often chosen at $\theta = 35^\circ$, but below we shall frequently denote waves with $\theta \approx 0^\circ$ as ‘the transverse waves’.

The far-field wave pattern is the sum of all wave components generated by different parts of the hull, progressing in various directions and interfering. The assumption of undisturbed base flow and small wave amplitudes is certainly satisfied in the far field. However, different potential fields are needed in the near field, since the superposition of wave components cannot be expected to satisfy the boundary condition on the ship hull. Moreover, the wave components propagating away from the hull pass through the curved flow field with variable velocity that prevails close to the hull, and thereby are affected by refraction, causing changes in wave amplitude, length and direction. Therefore, the pure superposition of sinusoidal waves can

only represent the wave pattern in the far field. Nevertheless, for general understanding, these refraction effects are of secondary importance.

The unique relation between wave direction, wave speed and wave length leaves only the amplitude and phase of the wave components in the far field as unknowns. In an expression for the free-wave pattern

$$\zeta(x, y) = \int_{-\frac{\pi}{2}}^{+\frac{\pi}{2}} \left[A(\theta) \cos \frac{g(x \cos \theta + y \sin \theta)}{V^2 \cos^2 \theta} + B(\theta) \sin \frac{g(x \cos \theta + y \sin \theta)}{V^2 \cos^2 \theta} \right] d\theta, \quad (5)$$

the amplitude and phase are determined by the functions $A(\theta)$ and $B(\theta)$, which represent the free wave spectrum. The wave resistance can then be expressed by:

$$R_w = \frac{1}{2} \pi \rho V^2 \int_{-\frac{\pi}{2}}^{+\frac{\pi}{2}} [A(\theta)^2 + B(\theta)^2] \cos^3 \theta d\theta. \quad (6)$$

Therefore the wave resistance depends quadratically on the wave amplitude, and there is a weighting factor $\cos^3 \theta$. The last result means that transverse waves are far more important for wave resistance than divergent waves, a significant finding for ship hull form design.

4 Outline of the approach

The procedure to analyse a ship wave pattern and to understand how it depends on the ship hull form is explained and illustrated more extensively in [9]. For completeness, in this section we summarise it.

We suppose that a computed wave pattern and flow field for an initial hull form at the desired speed are available, e.g. from a free-surface potential-flow or free-surface RANS computation. Alternatively, an observed or measured wave pattern would be useful, although, as will appear, availability of the (computed) hydrodynamic pressure distribution plays a central role in the analysis.

The analysis of the wave pattern and flow field evidently must start with identification of the dominant wave components. Referring to Eq. 6 we see that, for the wave resistance, ‘dominant’ means a large amplitude *and* a not too large angle θ , in view of the $\cos^3 \theta$ weighting factor. Because of their greater wave length, transverse waves may often be visually less apparent than the steeper, shorter diverging waves, but nevertheless they may be dominant for wave resistance.

To decide how to modify the hull form to reduce those dominant waves, one needs to identify which hull form aspects generate these, e.g. bow, stern, shoulders or

perhaps bow + fore shoulder, or a detail of a bulbous bow etc. Then those aspects can be adjusted in a way that reduces the amplitudes of these waves and improves their interference. However, in this step one needs to understand the connection between hull form and wave making. How can one guess which of the many different possible wave components is generated preferentially by a certain hull form feature? And what change should be applied to that feature?

To obtain an insight into the complicated relationship between hull form and wave making, it has been found useful in practice to make certain simplifications. These can be formally represented as a virtual distinction between two separate steps:

1. Consider the relation of the hull form with the hydrodynamic pressure distribution over the hull, and consider the association with the resulting pressure disturbance at the still-water surface
2. Estimate the wave-making properties of that still-water surface pressure distribution

For each of these steps, general guidelines can be derived fairly easily, and these will be summarised below.

Step 1: From hull form to free-surface pressure distribution The quantity to be considered first is the distribution over the hull surface of the hydrodynamic pressure coefficient. This pressure distribution is determined by the hull form and the ship speed, water depth etc. However, as we try to go step by step, wave effects are disregarded in this first step; this makes the hydrodynamic pressure coefficient independent of ship speed.

The relation between hull form and hull pressure distribution is described more completely in [9] and is only summarised here, as the following guidelines.

High pressures occur:

- Near stagnation points, in the bow area. In most cases there is also a pressure rise towards the stern, dependent on stern type and viscous effects.
- At concave streamwise curvatures: the centrifugal acceleration acting on the flow is balanced by a pressure rise away from the centre of curvature.
- At large streamwise slopes: a large angle of the streamlines relative to the longitudinal direction (outward on the forebody, inward on the aftbody) leads to a somewhat elevated pressure, as can be explained from the concavity of streamlines further from the hull.

Low pressures occur:

- At convex streamwise curvatures, again due to centrifugal acceleration.
- Due to displacement effect, the volume taken by the hull requiring a small speedup of the flow next to it.

Except for the stagnation point effect, the effect of streamwise curvature is by far the strongest in most practical ship hull cases.

These are, of course, well-known relations. Quantitative results can easily be obtained by making a double-body potential-flow computation.

The aspect of the pressure field around the hull that is most important for wave generation is the pressure distribution at the still-water surface. Therefore we have to assess that pressure distribution, again in connection with the hull shape. Suppose that a hull form feature causes a pressure variation on the hull in longitudinal direction at a certain depth, having a length scale L_p in that direction. Evidently this is accompanied by a pressure disturbance in the flow away from the hull and at the still-water surface—but with what properties? Here the following guidelines hold:

- The amplitude of the pressure disturbance decreases quickly with increasing distance/ L_p ; the length scale in longitudinal direction of the pressure disturbance increases with distance/ L_p .
- A short pressure variation on the hull thus has just a local effect on the pressure field; a longer pressure variation is felt at larger distances.
- Therefore, the pressure distribution on the still-water surface is caused by all hull pressure variations along the waterline, and by the larger-scale pressure variations farther beneath the water surface.
- Conversely, pressure variations at the water surface with small length scales can only be generated by form features close to the water surface.

Some illustrations will be provided in the next section.

Step 2: From free-surface pressure distribution to wave pattern We consider the wave pattern as driven by this hydrodynamic pressure distribution at the location of the still-water surface. From the dynamic free-surface boundary condition the wave elevation is $\zeta = \frac{1}{2}Fn^2L \cdot c_p$, but here we cannot simply use the double-body pressure coefficient: if, e.g. c_p is high on a part of the hull just below the water surface, this will generate a local wave crest plus a trailing wave system behind it. The question is what that wave system will look like: Which of the wave components generated will be significant and which will not?

The answer lies in the guideline:

- A wave is most effectively generated by a pressure variation of comparable length and shape.

Explanation and interpretations of this guideline are given below.

5 Discussion of the steps

The relation between hull form and wave making has thus been decomposed in two separate and fairly understandable steps. Now not only some more support may be needed for the guidelines given, but one may also wonder whether it is allowed at all to make this decomposition. Therefore, in the present section the different steps will be considered in more detail, illustrations will be given and restrictions and approximations indicated, while subsequent sections address the validity of the decomposition itself.

Step 1: From hull form to free-surface pressure distribution Figure 2 shows the pressure field for the KVLCC2 tanker in double-body flow. It illustrates well the various trends described: a high pressure around the bow and stern stagnation points, low pressures at all convex streamwise curvatures (fore and aft shoulder, transition to the bottom in the forebody, sides of stern gondola) and a small underpressure along the parallel midbody caused by the displacement effect. We also observe that pressure variations close to the waterline are continuous from hull to still-water surface, and that smaller-scale pressure variations further beneath the water surface, such as the low-pressure area at the stern gondola, have no visible effect at the still-water surface.

To support the guidelines for assessing the free-surface pressure field from the hull pressure distribution, let us first consider a point source of strength Q at position $(x_0, 0, z_0)$ in an undisturbed inflow V . As is well known, this produces a flow and pressure field corresponding with that around a semi-infinite body of revolution, a ‘Rankine half-body’. The dimensions of that body, and the length

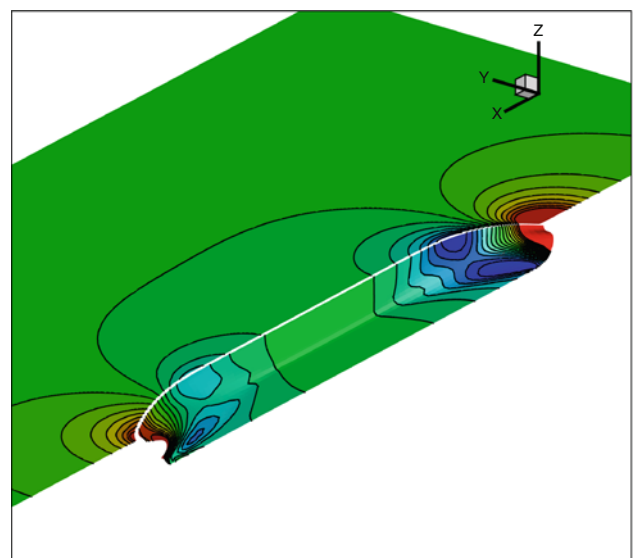


Fig. 2 Double-body pressure distribution for KVLCC2 tanker

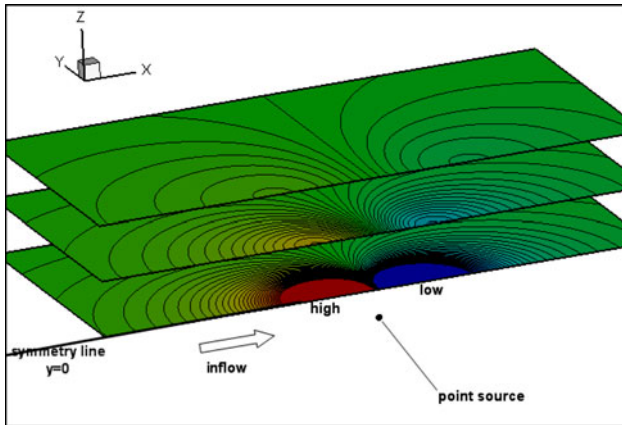


Fig. 3 Pressure field induced by a point source in a uniform inflow in x -direction. The source induces a pressure variation at the still-water surface with a maximum and minimum pressure. The three planes show the pressure pattern (starboard half only) at the still-water surface for submergence depths of the source equal to L_p , $3L_p$ and $5L_p$ [9]

scale of the pressure variation over it, are proportional to $L_p = \sqrt{Q/(4\pi V)}$. The resulting pressure variation at the still-water surface in double-body flow can be approximated (linearised) as:

$$c_p = -4 \frac{L_p^2}{R^2} \cdot \frac{x - x_0}{R} \tag{7}$$

for a point at the still-water surface at a distance R from the source. So, the pressure amplitude at the still-water surface decays proportional to $(L_p/R)^2$, while the length scale increases linearly with R/L_p . Figure 3 illustrates this behaviour. Wave patterns generated by such submerged point sources will be shown in the next subsection.

Therefore, for this isolated source, the first two guidelines given are confirmed. For other perturbations the decay of the pressure amplitude can be different, but in the far field in three dimensions (3D) the decay is still proportional to $(L_p/R)^2$ or even quicker.

To elaborate on the second guideline, i.e. ‘A short pressure variation on the hull has just a local effect on the pressure field; a longer pressure variation is felt at larger distances’, Fig. 4 shows two examples of the pressure field around an array of 10 equal point sources on the x -axis. The first graph is for closely spaced sources, giving a short pressure variation; in the second graph the sources are spread out over the interval $[-4.5, 4.5]$, and the length scale of the pressure variation is larger. The source strengths are such that an equal pressure amplitude is generated at the lower boundary $z = 2.2$ for both cases. However, due to the greater length scale, at larger distance the pressure amplitude is twice as large for the second case, illustrating that longer pressure variations extend to larger distances.

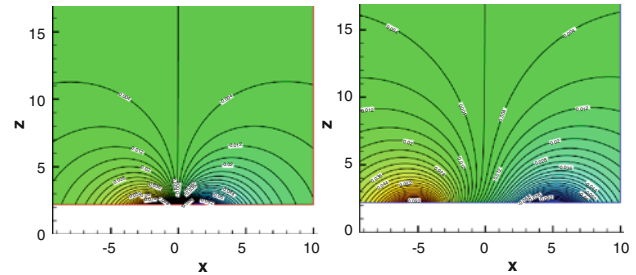


Fig. 4 Pressure field around source array. *Left* short pressure variation, *right* longer pressure variation with equal amplitude

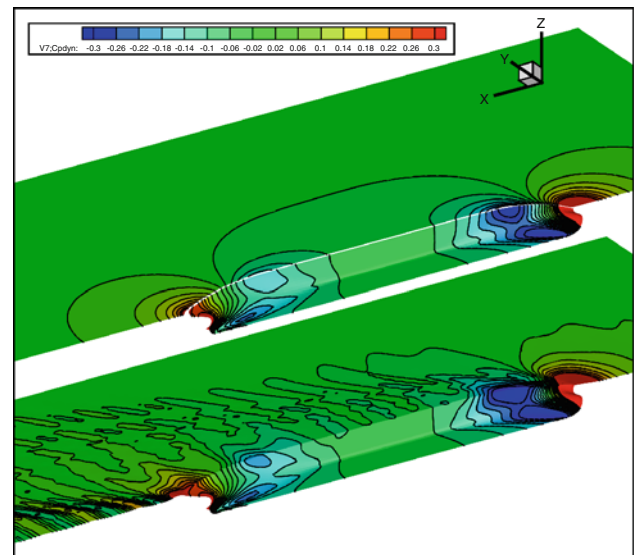


Fig. 5 Hydrodynamic pressure distribution for KVLCC2 tanker, in double-body flow (*top*) and free-surface flow (*bottom*)

Thus, the guidelines provided for step 1, relating the pressure field with the hull form, are fairly evident. However, the objection could be raised that we have not considered the effect of the free water surface at all in addressing the relation between hull form and pressure distribution. We have simply used a pressure distribution in double-body flow, but is that still relevant to explain wave making? Or is the pressure field including the waves entirely different?

The answer evidently depends on the Froude number, since the double-body flow can be considered to be the limit of free-surface flow for $Fn \rightarrow 0$. We show some examples to illustrate the level of correspondence. Figure 5 compares the double-body and free-surface pressure distributions, on hull and water surface, for the KVLCC2 tanker model. The free-surface case is for $Fn = 0.1423$. Obviously there is a large degree of correspondence between the hull pressure distributions. However, there is an increase of the underpressures close to the water surface as a result of free-surface effects, clearly observable at the

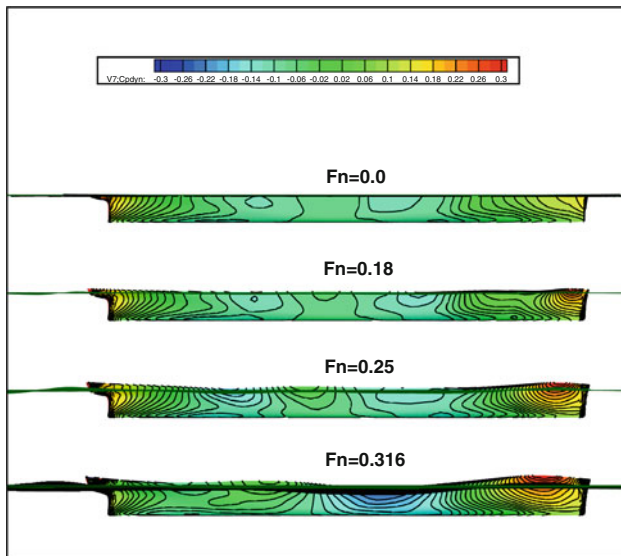


Fig. 6 Hydrodynamic pressure distribution for Series 60 $C_B = 0.60$ hull, in double-body flow (*top*) and at different Froude numbers

fore and aft shoulder. There is no apparent change of the pressure at the stern gondola. This increase of the pressure extremes, in particular the underpressures, close to the water surface is a very common observation. Nevertheless, in general the distributions remain similar.

Figure 6 makes a similar comparison for the Series 60 $C_B = 0.60$ hull, at Froude numbers 0.0 (double-body), 0.18, 0.25 and 0.316. We see that many of the features of the hull pressure distribution are kept for increasing speed. However, there is a clear increase of the overpressure at the bow, which also shifts aft with increasing speed. The underpressure at the fore shoulder is also augmented by the free-surface effects, and is in addition affected by interference with the bow wave system, in particular at $Fn = 0.18$ and $Fn = 0.316$. The aft shoulder underpressure shows similar effects and tends to move gradually aft with increasing speed, interference again playing a role. We notice that further aft there is a greater Fn dependence, due to the cumulative effect of waves generated further upstream. Like in the previous case, the pressure distribution in double-body flow still gives a good impression of the pressure distribution in free-surface flows, as long as the wave making and wave interference are not too pronounced.

In general, the connection that step 1 makes between the hull form and pressure distribution, regardless of free-surface effects, seems a useful approximation for most merchant vessels at usual Froude numbers. However, the free surface usually increases the pressure extremes and causes a slight aft shift of these. Besides, the wave pattern generated at some point along the hull causes an oscillating pressure field further aft.

Evidently, at higher Fn and more pronounced wave making the agreement will be worse, and the pressure distribution is not as easily explained in terms of the hull form only. Moreover, there are some hull form features for which double-body flow is substantially different from free-surface flow. For example, for a bulbous bow extending just beneath the still-water surface, in double-body flow the flow has to pass horizontally over the bulb and through the narrow gap between the bulb and its mirror image; this can generate extreme pressure variations that are largely absent in free-surface flow as the flow direction is different. Also for immersed transom sterns, there are locally substantial differences in pressure distribution between double-body and free-surface flow. In such cases the double-body pressure distribution is still connected with the hull form as usual, but is less relevant for the wave making.

Therefore, in practice we normally analyse the hull pressure distribution from a free-surface potential-flow computation, rather than that from double-body flow, keeping in mind the effect of the free surface on the magnitude and position of pressure extremes. With experience this somewhat less formal procedure works well.

Step 2: From free-surface pressure distribution to wave pattern The guideline given above was: ‘A wave is most effectively generated by a pressure variation of comparable length and shape’. This tells us that a wavy pressure distribution moving over the still-water surface will preferentially generate waves that have a comparable wave length. The condition of corresponding shape applies to both the longitudinal and transverse directions.

To illustrate what this means, Figs. 7 and 8 show a variety of wave patterns generated by synthetic pressure distributions acting on the free surface of an inflow with speed V . The imposed pressure distributions are sinusoidal in longitudinal direction, with a single period over a length L_p , and constant with smoothed sides in transverse direction, with width B_p . The pressure is given by:

$$p(x - x_0, y - y_0) = P \cdot \sin\left(\frac{2\pi(x - x_0)}{L_p}\right) \cdot f(y - y_0)$$

$$\text{for } -0.5L_p < x - x_0 < 0.5L_p,$$

in which $f(y) = 1.0$ for $|y| < 0.25B_p$ and

$$f(y) = \cos^2\left[\frac{2\pi(y - 0.25B_p)}{B_p}\right] \text{ for } 0.25B_p < |y| < 0.5B_p.$$

For a given speed, the length L_p and width B_p of the pressure distribution have been varied to study the resulting wave pattern. The dimensions of the pressure patch are here given as fractions of the transverse wave length λ_0 for the speed considered.

Figure 7 shows how the wave pattern responds to variations of the length of the pressure patch (with a sinusoidal shape over that length), at constant width $B_p = \lambda_0$. The top

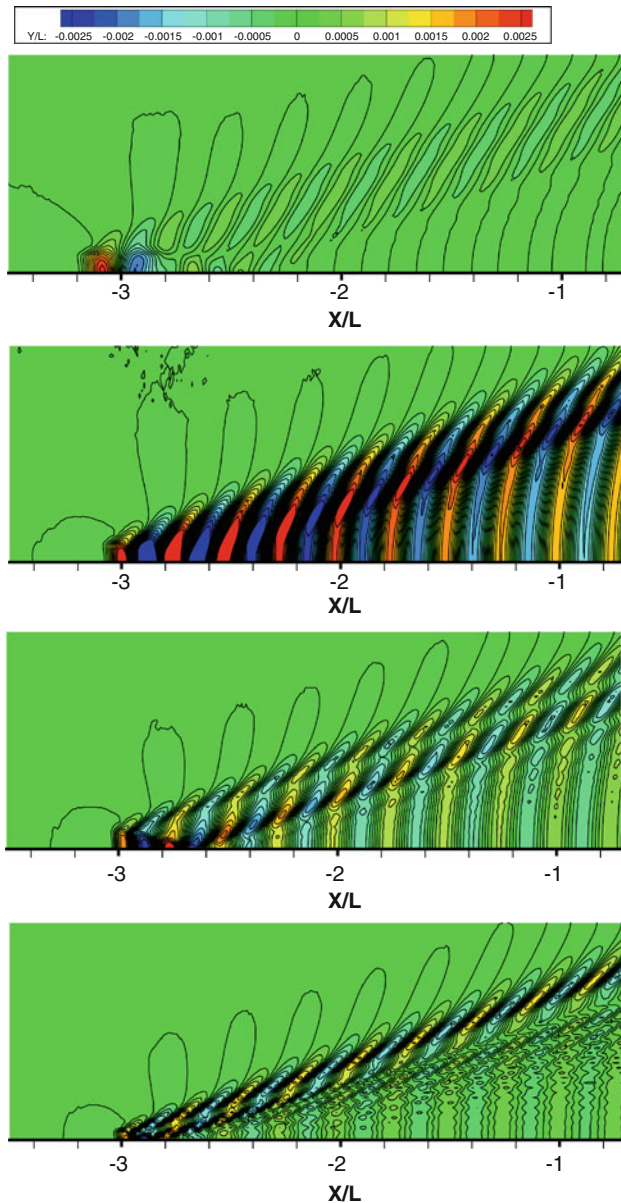


Fig. 7 Wave patterns generated by travelling pressure patches. *Top* width $B_p = \lambda_0$, length $L_p = 2\lambda_0$; *Second graph* width λ_0 , length λ_0 ; *Third graph* width λ_0 , length $0.5\lambda_0$; *Bottom graph* width $0.5\lambda_0$, length $0.5\lambda_0$

figure is for a pressure patch length $L_p = 2\lambda_0$. As the transverse wave is the longest possible wave in the steady pattern, this pressure distribution fits no wave well, and the wave amplitudes are very limited, waves being mostly generated by the sides of the pressure patch. The second graph is for a pressure distribution with $L_p = \lambda_0$, which fits a transverse wave precisely and thus appears to generate a system with pronounced transverse waves and a limited amount of somewhat more diverging components. In the third graph, for $L_p = 0.5\lambda_0$, the transverse components have decreased strongly and diverging waves are more

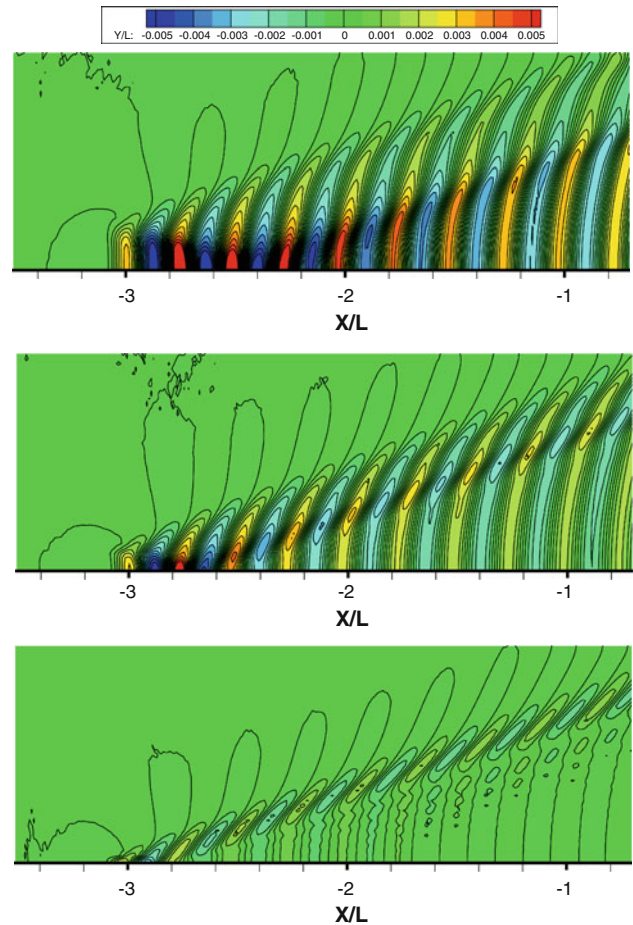


Fig. 8 Wave patterns generated by travelling pressure patches, with length $L_p = \lambda_0$ and widths $B_p = 2\lambda_0$, λ_0 and $0.25\lambda_0$ (*top to bottom*)

pronounced, as these fit the longitudinal distribution well, being shorter by a factor of $\cos \theta$ if measured in longitudinal direction. When next also the width of the pressure patch is halved to $B_p = 0.5\lambda_0$ (fourth graph), the diverging waves fit even better and are still more dominant.

Figure 8 shows the wave patterns of pressure patches with fixed length $L_p = \lambda_0$ and varying widths. One might expect dominance of transverse waves in all cases, but the width of the pressure distribution appears to matter as well. In the first graph, for $B_p = 2\lambda_0$, there are just transverse waves and very little else. Halving the pressure width to λ_0 still gives dominant transverse waves, but somewhat weaker. If the width of the pressure patch is reduced to $0.25\lambda_0$ (Fig. 8 third graph), transverse waves are still there but much lower; diverging components are dominant in amplitude, as they fit well this small width.

Therefore, the guideline given above well indicates the wave patterns generated by free-surface pressure distributions. Both the transverse and the longitudinal extent matter, and the more localised a pressure disturbance is, in length and width, the more it tends to generate diverging

waves. Anticipating qualitatively the type of wave pattern from a simple free-surface pressure distribution is relatively straightforward. Moreover, owing to the link between the flow around the hull and the free-surface pressure distribution, anticipating the wave pattern from a ship hull shape has got a rational basis, which is the main objective of the analysis procedure.

Of course the guideline for step 2 is in itself nothing new. There have been several studies of wave making caused by surface pressure disturbances, e.g. [13, 14]. Linear theory provides analytical expressions for the wave pattern [15] which indicate that the amplitude of waves generated in direction θ is proportional to the 2D Fourier transform of the distribution of the longitudinal pressure derivative at the wavenumber of those waves. Referring to the wave height expression for the far field (Eq. 5), the expression is:

$$A(\theta) + iB(\theta) = -\frac{\sec^3 \theta}{\pi \rho V^2} \iint_{FS} \frac{\partial p}{\partial x} \exp \left[\frac{ig(x \cos \theta + y \sin \theta)}{V^2 \cos^2 \theta} \right] dx dy. \quad (8)$$

This confirms that a pressure distribution with a length scale and shape matching the wave components produces the largest wave amplitudes. Therefore, the simple rule given above is actually precise in case of pressure distributions of infinite extent.

As a first illustration of the results of the combination of both steps, we inspect the wave pattern generated by the still-water surface pressure distribution as in Eq. 7, thus approximating the wave pattern of a submerged point source. Figure 9 shows that pattern for submergences of 5, 4 and 3 times the length scale associated with the point source. Defining the length scale of the pressure distribution at the still-water surface as twice the distance between maximum and minimum pressure, for a submergence of $5L_p$ this is close to λ_0 for the speed considered. The result is the generation of a weak transverse wave system. If the submergence is reduced, the amplitude of the pressure disturbance increases quickly, but also the length scale of the surface pressure distribution gradually decreases. Consequently, the amplitude of all waves increases, but the rapid increase of the diverging wave components is more evident. This supports the guideline that:

- Deeply submerged pressure disturbances can only generate longer waves; shallow pressure disturbances can generate also shorter waves.

Because of its analytical background, also the second step in the procedure may seem absolutely sound, but again there is an important possible objection to its use in the present context: the waves generated by the surface pressure field are

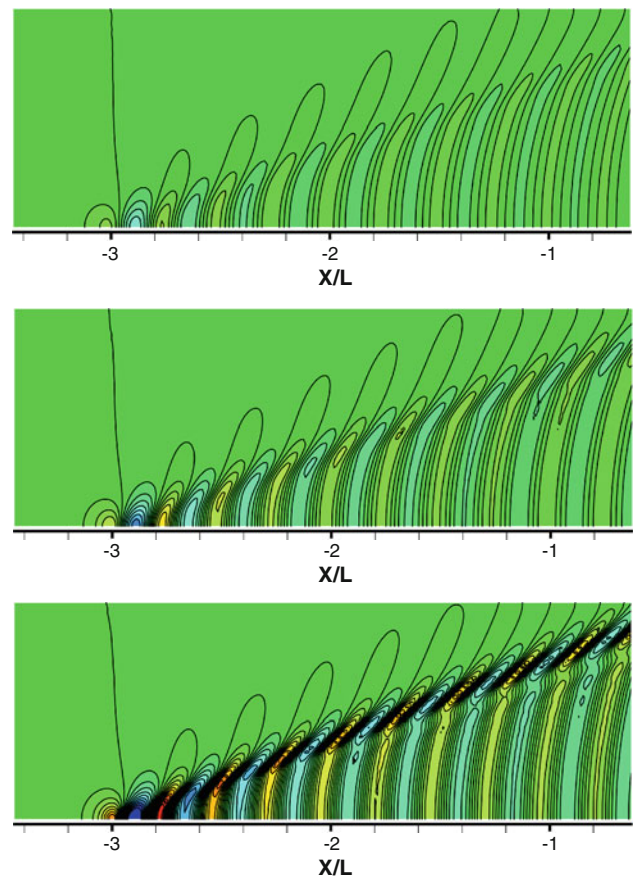


Fig. 9 Wave patterns generated by a submerged point source, at submergence of 5, 4 and $3L_p$ (top to bottom)

computed while disregarding the presence of the ship hull. In reality the hull boundary condition must modify the waves in the near field. Moreover, the waves do not propagate through still water, but through the curved flow field with variable velocity around the hull. This produces changes in the dispersion relation, and refraction effects that modify the wave lengths, directions and amplitudes. One result is the apparent forward shift of the Kelvin wedge of a ship’s bow wave system, but also the strength of diverging wave components is affected by these effects [16]. However, the resulting differences are not too substantial for the dominant waves in the pattern, so for the qualitative analysis and understanding that we aim at, the approximation is applicable.

6 Relation with ship wave theories

While the discussions above may be physically plausible, some stronger theoretical foundation is desired. In fact, related theoretical two-step approaches have already been proposed in the past, albeit with a different objective. Specifically the procedure is very much in the spirit of slow-ship theory, as demonstrated below.

Let us first indicate the form of the free-surface boundary conditions for a potential flow with an imposed free-surface pressure field. The kinematic and dynamic free-surface boundary conditions, nondimensionalised with ship speed and length, read:

$$\phi_x \zeta_x + \phi_y \zeta_y - \phi_z = 0 \quad \text{at } z = \zeta(x, y), \tag{9}$$

$$\frac{1}{2}Fn^2(1 - \phi_x^2 - \phi_y^2 - \phi_z^2) - \frac{1}{2}Fn^2 c_p(x, y) - \zeta = 0 \tag{10}$$

at $z = \zeta(x, y)$,

in which $c_p(x, y) \equiv p(x, y)/(\frac{1}{2}\rho V^2)$ is the nondimensional pressure distribution imposed at the free surface. A combined form of both conditions is thus obtained:

$$\begin{aligned} &\frac{1}{2}Fn^2 \left(\phi_x \frac{\partial}{\partial x} + \phi_y \frac{\partial}{\partial y} \right) (\phi_x^2 + \phi_y^2 + \phi_z^2) + \phi_z \\ &= -\frac{1}{2}Fn^2 \left(\phi_x \frac{\partial}{\partial x} + \phi_y \frac{\partial}{\partial y} \right) c_p \quad \text{at } z = \zeta(x, y). \end{aligned} \tag{11}$$

We see that the imposed pressure distribution provides a forcing term on the right-hand side in the combined free-surface boundary condition, representing the streamwise derivative of the imposed free-surface pressure.

Next, we consider wave making by a ship, without any free-surface pressure distribution. The flow is determined by the nonlinear boundary conditions 9 and 10 without the c_p contribution, and by a body boundary condition. As mentioned, in the past various linearised formulations have been proposed, and one of the more successful ones was the so-called slow-ship linearisation or double-body linearisation, used in e.g. Dawson’s method [1]. It is based on the assumption that the flow with free surface is a small perturbation of the flow without free surface around the hull, i.e. the double-body flow. The potential is then decomposed as:

$$\phi(x, y, z) = \Phi(x, y, z) + \phi'(x, y, z), \tag{12}$$

where $\nabla\Phi$ is the double-body flow velocity, and we assume that the perturbation velocity $\nabla\phi' = \mathcal{O}(Fn^2) \ll 1$ at the free surface. While there has been some debate on the proper form of the free-surface boundary condition, a usual version as derived e.g. in [17], is

$$\begin{aligned} &Fn^2(\Phi_x^2 \phi'_{xx} + 2\Phi_x \Phi_y \phi'_{xy} + \Phi_y^2 \phi'_{yy}) + \phi'_z \\ &= (\Phi_x \zeta_r)_x + (\Phi_y \zeta_r)_y, \end{aligned} \tag{13}$$

which is to be imposed at $z = \zeta_r(x, z) \equiv \frac{1}{2}Fn^2(1 - \nabla\Phi \cdot \nabla\Phi)$.

Therefore, the right-hand side can be written as

$$\frac{1}{2}Fn^2 \left(\Phi_x \frac{\partial}{\partial x} + \Phi_y \frac{\partial}{\partial y} \right) \left(\frac{\zeta_r}{\frac{1}{2}Fn^2} \right) - \Phi_{zz} \zeta_r.$$

If we compare this expression with Eq. 11, we see that, save for the second term which is a ‘transfer term’ approximating Φ_z at $z = \zeta_r$, it corresponds precisely with

the forcing by an imposed pressure distribution. Comparing the form of the free-surface boundary conditions we see that, in slow-ship theory, the wave pattern is considered as generated by a free-surface pressure distribution

$$c_p(x, y) = -\frac{\zeta_r}{\frac{1}{2}Fn^2},$$

which is the negative of the pressure found in double-body flow at the still-water surface. The minus sign can be understood from the fact that a high pressure at the still-water surface in double-body flow generates a positive local wave elevation; to get the same wave elevation without the hull being present, we have to impose the opposite of that pressure on the water surface.

The distinction of the two steps, and the use of the free-surface pressure distribution from double-body flow to determine the wave generation, thus agrees with slow-ship theory, and just like in our procedure, two steps have to be made to apply slow-ship theory methods. However, an essential feature of slow-ship theory was the fact that in that second step the wave propagation over the curved and variable double-body flow field (which determines the variable coefficients at the left hand side) was taken into account. This is an aspect that we disregard in our approximate procedure, but again, our aim is understanding not predicting.

Moreover, in most of the slow-ship methods also the hull boundary condition was taken into account in the second step. On the other hand, in earlier methods more analytical techniques were attempted, and the hull boundary condition was sometimes disregarded in the wave pattern prediction. Baba and Takekuma [18, 19] actually derive the same slow-ship boundary condition, and solve the wave pattern as if generated by the opposite of the double-body free-surface pressure distribution in the absence of the ship hull. In the derivation the nonuniformity of the double-body flow is taken into account, but their expression for the far-field wave pattern is actually equal to that for a pressure distribution in an undisturbed flow [15], the nonuniformity of the flow only remaining in the expression for the free-surface pressure itself.

Another comparable procedure is discussed by Lighthill [20]. Again, the flow field is thought to be composed of a double-body flow field and a resulting wave disturbance. The double-body flow field causes a pressure variation over the still-water surface, which again generates the wave pattern. However, in this reference there is no derivation, and no discussion of the disregarded effects of the non-uniformity of the flow; the purpose in his book again is understanding rather than prediction.

In any case, the two-step procedure proposed here appears to be related with slow-ship theory in general, and with some of the earlier versions, such as that by Baba and Takekuma, in particular. Here one might suppose that this

would limit the applicability of our approach to low Froude numbers only, since slow-ship theory is asymptotically valid for $Fn \rightarrow 0$. However, from experience with e.g. Dawson's method it is known that, in practice, this linearisation works fairly well for most merchant vessels and is not confined to low speeds only. Even so, the simplified slow-ship methods mentioned, and the additional simplifications we make, e.g. disregarding the hull boundary condition for the waves and neglecting the effect of the double-body flow nonuniformity on the wave propagation, may ask for some further validation.

7 Validation of the two-step approach

As we have pointed out, the two steps distinguished in our procedure separate physical effects that in fact are occurring together and interact. Evidently, mutual influences are thus omitted. One may wonder whether this still leads to the right conclusions on the relation of hull form and wave pattern.

The previous section has shown that there is a strong relation of the two-step approach advocated here with early slow-ship linearised ship wave-making theories. Therefore, a global validation is possible by evaluating the wave making of ships by those methods. However, we do not need to follow the methods very precisely, as some of their simplifications were required by the computational possibilities at the time of development. Therefore, what we will do is the following:

- Compute the double-body flow around a ship hull, using a usual panel code essentially following the method of Hess and Smith [21].
- Evaluate the resulting pressure distribution $p(x, y)$ at the still-water surface around the hull, from the velocities found in a dense net of 'offbody points' on the still-water surface.
- Impose the opposite of that pressure distribution, $-p(x, y)$, on the free surface and compute the wave pattern generated by it, in the absence of the ship hull. We simply use here the nonlinear potential flow solver, not any linearised formulation, as it is available and very fast.

The question arises of what to do with the waterplane area of the ship. This part of the water surface in the wave pattern computation is internal to the hull in the double-body flow computation, so we do not have a pressure distribution here. Various choices have been made in the past: Baba and Takekuma impose no pressure in this area, while Lighthill suggests to extrapolate the pressure field next to the ship inside it, i.e. for a symmetric case the pressure is largely constant in transverse direction across

the waterplane area. In some first evaluations we found that the latter model leads to exaggerated transverse waves. This can be understood if we imagine a very shallow, very wide ship hull: any local pressure at the waterline would then be modelled as a wide pressure strip across the beam of the hull, which would have much too large an effect on transverse wave making. In the examples shown below we have therefore not imposed any pressure in the area of the ship waterplane itself, just the pressure field surrounding it.

In this way we obtain a prediction of the wave pattern subject to the same assumptions and simplifications as underlie the analysis approach. We will compare that wave pattern with the ship wave pattern predicted directly by the nonlinear free-surface potential flow code RAPID, in which these approximations are not made; thus we get direct information on the importance of the approximations. Moreover, we compare with experimental data.

The first case is the Series 60 $C_B = 0.60$ model at $Fn = 0.316$. Figure 10 compares the wave pattern so obtained for the pressure distribution with that of the ship hull itself. The agreement is remarkable. The wave cuts at $y/L = 0.2067$ shown in Fig. 11 show that the approximate procedure actually predicts the same type of waves for this case, but with small differences in phase and amplitude.

Figure 12 shows a similar comparison for the Kriso Container Ship, a benchmark case with bulbous bow and transom stern. The differences are perhaps somewhat larger here, mainly in the amplitude of diverging bow waves, but the main features of the wave pattern, and the essence of what is needed in order to understand the relation between hull form and wave pattern, are again well represented. The wave cut in Fig. 13 shows good correspondence with the result of the complete nonlinear prediction, which is in very good agreement with the experimental data.

The last comparison we show is for the 'Hamburg Test Case', a containership, at $Fn = 0.238$. Figure 14 shows the

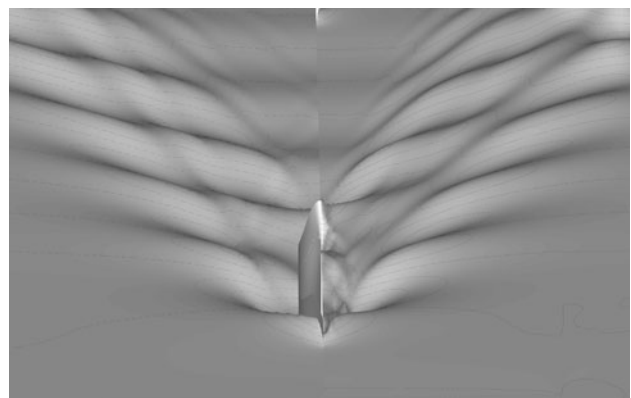


Fig. 10 Computed wave patterns, of Series 60 $C_B = 0.60$ at $Fn = 0.316$ (left side), and of its double-body pressure field moving at the same speed over the still-water surface (right side), in a perspective view from ahead

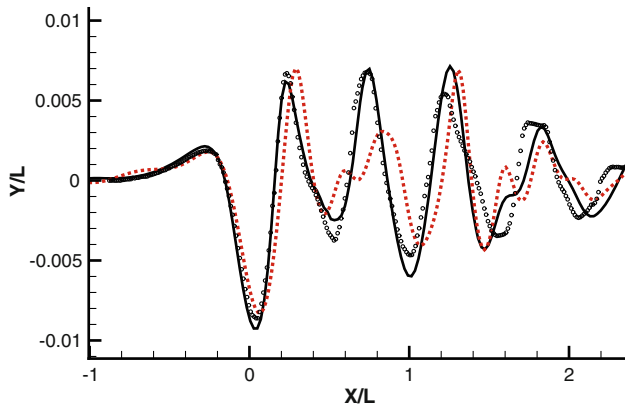


Fig. 11 Computed wave cuts at $y/L = 0.2067$, for Series 60 $C_B = 0.60$ at $Fn = 0.316$ (full line), and of its double-body pressure field moving at the same speed over the still-water surface (dotted line), and experimental data [22] (markers)

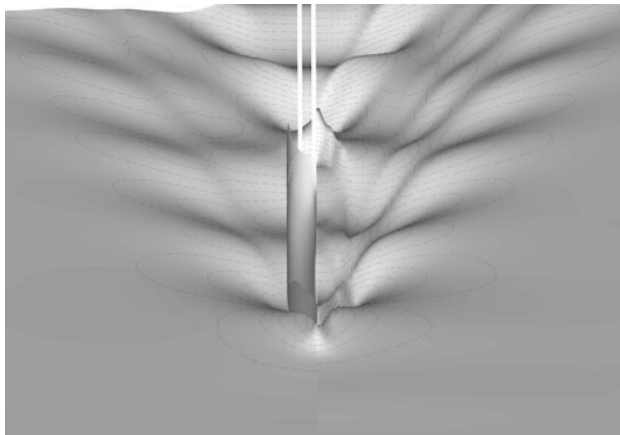


Fig. 12 Perspective view of computed wave patterns, of the Kriso Container Ship (KCS) at $Fn = 0.26$ (left side), and of its double-body pressure field moving at the same speed over the still-water surface (right side)

wave patterns and Fig. 15 the wave cuts, again with experimental data. While there is no doubt that the predictions from the complete free-surface panel method are better, the ability of the two-step approach to represent the main features of the wave pattern is evident.

We note in passing that the Froude numbers for these examples differ, but there is no indication that the slow-ship-like method used works better for lower than for higher Fn ; other aspects of the particular case dominate. From a number of such comparisons we have observed that larger deviations occur in cases with large bulbous bows very close to the water surface, or with immersed transom sterns. In both cases the double-body flow gives no adequate representation of the local pressure field. Therefore, for qualitative understanding of the wave making, inspection of the hull pressure distribution from a free-surface potential flow computation may actually be preferable, at least in such cases.

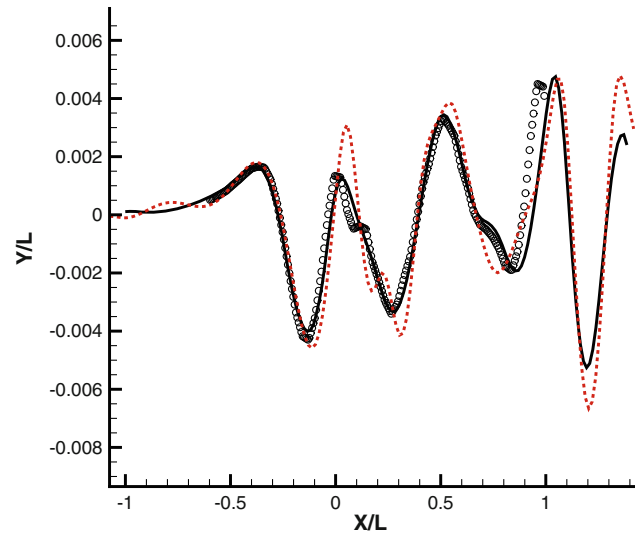


Fig. 13 Computed wave cuts at $y/L = 0.1509$, for KCS model at $Fn = 0.26$ (full line), and of its double-body pressure field moving at the same speed over the still-water surface (dotted line). The markers represent experimental data

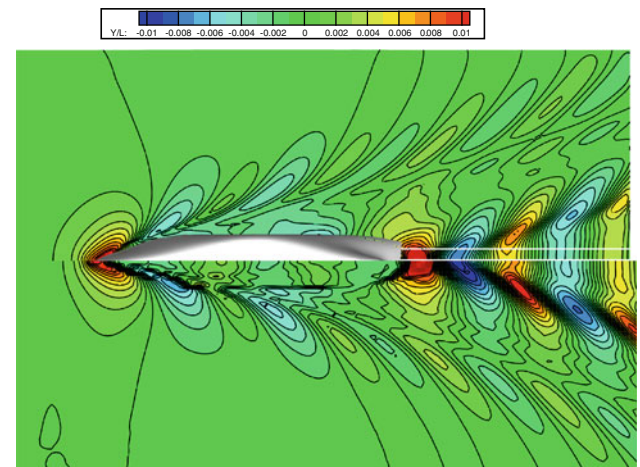


Fig. 14 Computed wave patterns, of the Hamburg Test Case at $Fn = 0.238$ (upper half), and of its double-body pressure field moving at the same speed over the still-water surface (lower half)

Overall we believe that the agreement of the wave patterns found by the simplified, two-step approach with those from a complete wave pattern prediction is striking and supports the adequacy of the simple analysis procedure proposed here.

8 Applications

The general philosophy outlined above enables us to understand and foresee a variety of, partly well-known, properties of ship wave making and design trends. We mention just a few points below to illustrate the use of the approach; Ref. [9] gives several additional examples.

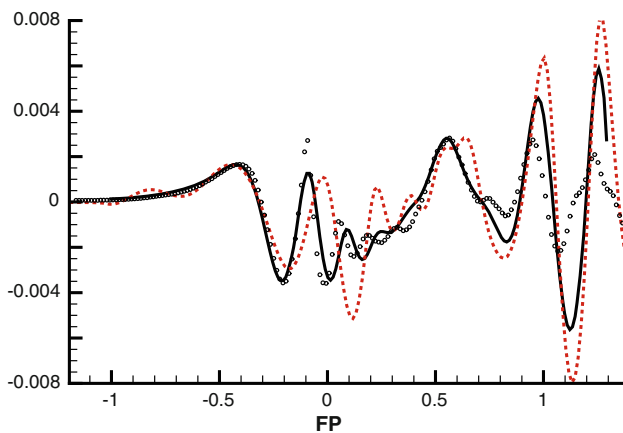


Fig. 15 Computed wave cuts at $y/L = 0.184$, for the Hamburg Test Case at $Fn = 0.238$ (full line), and of its double-body pressure field moving at the same speed over the still-water surface (dashed line). The markers represent experimental data

- Transverse waves have the largest weighting factor in the resistance expression. Transverse waves are strongest if the free-surface pressure distribution has a length scale matching those waves, i.e. $L_p \approx \lambda_0$. For the significant, overall pressure variation along the hull spanning from bow to stern, this is the case at $Fn \approx 0.4$, which is the explanation of the primary resistance hump.
- The overpressure around the bow stagnation point is rather extensive for a blunt bow and induces a pressure at the still-water surface over a wider area, whereas for a sharp bow it is more localised in length and width. Therefore, a sharp bow generates more diverging bow waves than a blunt bow.
- A wide, flat transom stern tends to generate transverse waves due to the width of the pressure disturbance it creates. However, the corners of a transom stern are local pressure disturbances creating sharply diverging waves.
- A catamaran generates stronger transverse waves than one would expect from the slenderness of its side hulls, due to the larger transverse extent.
- A submarine at some distance under the surface cannot generate diverging waves, as there are no short scales in the surface pressure disturbance.
- At low Fn , all possible waves are relatively short, and respond to short surface pressure disturbances which can only be induced by near-surface hull form features. Therefore, it is the waterline shape that counts. However, at higher Fn the waves are generated by larger length scales that are also affected by form features farther beneath the surface, and the sectional area curve becomes more important.

- Localised hull form features far beneath the water surface (e.g. stern bulbs) are generally insignificant for wave making.
- While one wants to avoid matching of a pressure length scale with a wave to minimise wave making, the opposite is the case if one wants to design a hull form modification to suppress a given wave. If a certain dominant wave is observed in a computed or measured wave pattern and it needs to be reduced, one should aim at making a hull form modification that creates a pressure change with a length scale comparable to that wave.
- Design trends for bulbous bows can be understood from the desired matching of length scales, the guidelines on the relation of the surface pressure distribution with the hull pressure distribution etc.

Furthermore, the general notions following from the approach described play an important role in the improvement of hull designs in practical applications. The practice we use is that first a computation is made for an initial hull form, normally using a free-surface potential flow code. In a careful analysis of the computed wave pattern, in combination with the hull pressure distribution found from the same (free-surface) computation, the guidelines and insights summarised in Sect. 4 and several others are used to relate the dominant wave components with hull form features, and to decide on hull form modifications that would reduce those waves. Next, these modifications are again evaluated by a fully nonlinear free-surface potential flow computation, if not a free-surface viscous-flow computation. After that, a next analysis and improvement step can be made. In just a few directed design steps a substantial reduction of wave making and wave resistance can often be achieved. Similarly, the same insights have proven successful in the context of a systematic hull form variation procedure to achieve wave resistance reduction [7, 8].

9 Conclusions

The main question addressed in the present paper is: What is the relation between hull form properties and ship wave patterns? The approach advocated here, which is a formalisation of a way of working developed at MARIN in the course of many years, decomposes this into two steps: the relation between ship hull form and free-surface pressure distribution, and the relation between that pressure distribution and the wave pattern it generates. The separate steps have been discussed and illustrated. Main conclusions can be summarised as follows:

- The advantage of the decomposition into two steps is that each of these is ruled by a few simple and understandable relations as listed in Sect. 4. Anticipating the wave pattern generated by a hull-induced surface pressure distribution is much more straightforward than anticipating the wave pattern of a ship.
- The two-step approach proposed here is closely related with the former ‘slow-ship linearised theory’, but has additional approximations as it does not pay attention to the propagation of waves over the flow field around the hull, and to the effect of the hull boundary condition on the waves. These simplifications are, however, essential for conceptual simplicity, and have been found to be permissible for the present purpose. The analysis approach has been found to be applicable to ships at normal displacement speeds, not only slow ships.
- In computational studies we have observed that a strict computational equivalent of the general approach predicts wave patterns that correspond at least qualitatively with the wave pattern according to a full nonlinear theory, and with experimental data. While it is not meant to propose an alternative prediction method, this lends support to the use of the method for analysing ship wave patterns and their dependence on hull form.

Evidently, applying these insights to improve ship hull forms from a wave-making point of view still remains an art, and substantial experience and feeling are still needed. However, a sound qualitative understanding of the physics allows one to make directed steps towards an improved hull form. Thus, a simplified analysis helps to achieve good results in a process based on advanced computational tools. To advocate this combination was an objective of this paper.

Acknowledgments The permission from the Society of Naval Architects and Marine Engineers (SNAME) to reproduce some material from [9] in this paper is acknowledged.

References

1. Dawson CW (1977) A practical computer method for solving ship-wave problems. In: 2nd International Conference on Numerical Ship Hydrodynamics, Berkeley, USA
2. Jensen G (1988) Berechnung der stationären Potentialströmung um ein Schiff unter Berücksichtigung der nichtlinearen Randbedingung an der Wasseroberfläche. Ph.D. Thesis, University of Hamburg, IfS Bericht 484
3. Janson C-E (1997) Potential flow panel methods for the calculation of free-surface flows with lift. Thesis, Chalmers Univ. Gothenburg
4. Raven HC (1992) A practical nonlinear method for calculating ship wavemaking and wave resistance. In: 19th Symposium on Naval Hydrodynamics, Seoul, South Korea
5. Raven HC (1996) A solution method for the nonlinear ship wave resistance problem. PhD Thesis, MARIN/Delft University of Technology, The Netherlands
6. Janson C-E, Larsson L (1996) A method for the optimization of ship hull forms from a resistance point of view. In: 21st Symposium on Naval Hydrodynamics, Trondheim, Norway
7. Valdenazzi F, Harries S, Janson CE, Leer-Andersen M, Marzi J, Maisonneuve JJ, Raven HC (2003) The FANTASTIC RoRo: CFD optimisation of the forebody and its experimental verification. NAV 2003 Symposium, Palermo, Italy
8. Hoekstra M, Raven HC (2003) A practical approach to constrained hydrodynamic optimization of ships. NAV 2003 Symposium, Palermo, Italy
9. Larsson L, Raven HC (2010) Ship resistance and flow. In: Paulling JR (ed) Principles of naval architecture series. Society of Naval Architects and Marine Engineers (SNAME), Jersey City, USA
10. Raven HC (1988) Variations on a theme by Dawson. In: Proceedings of the 17th Symposium Naval Hydrodynamics, Den Haag, Netherlands
11. Raven HC (1998) Inviscid calculations of ship wavemaking—capabilities, limitations and prospects. In: 22nd Symposium Naval Hydrodynamics, Washington, DC, USA
12. Newman JN (1977) Marine hydrodynamics. MIT Press, Cambridge
13. Tuck EO, Scullen DC, Lazauskas L (2002) Wave patterns and minimum wave resistance for high-speed vessels. In: 24th Symposium on Naval Hydrodynamics, Fukuoka, Japan
14. Doctors LJ (1997) Optimal pressure distributions for river-based air-cushion vehicles. Schiffstechnik 44
15. Wehausen JV, Laitone EV (1960) Surface waves. In: Encyclopedia of Physics, vol IX, Springer, pp 446–778
16. Raven HC (1997) The nature of nonlinear effects in ship wavemaking. Ship Technol Res 44(1):134
17. Newman JN (1976) Linearized wave resistance theory. International Seminar on Wave Resistance, Tokyo/Osaka, Society of Naval Architects Japan
18. Baba E, Takekuma K (1975) A study on free-surface flow around bow of slowly moving full forms. J Soc Naval Archit Jpn 137:65–73
19. Baba E, Hara M (1977) Numerical evaluation of a wave-resistance theory for slow ships. In: 2nd International Conference on Numerical Ship Hydrodynamics, Berkeley, USA
20. Lighthill J (1980) Waves in fluids. Cambridge University Press, Cambridge
21. Hess JL, Smith AMO (1962) Calculation of non-lifting potential flow about arbitrary three-dimensional bodies. Douglas Aircraft Company, Report No. 40622
22. Toda Y, Stern F, Longo J (1991) Mean-flow measurements in the boundary layer and wake and wave field of a Series 60 $C_b = .6$ ship model for Froude numbers .16 and .316. IIHR Report No. 352, Iowa Institute of Hydraulic Research, Iowa, USA